Molecular Microbiology (2004) **53**(6), 1771–1783 doi:10.1111/j.1365-2958.2004.04242.x

Complex spatial distribution and dynamics of an abundant *Escherichia coli* outer membrane protein, LamB

Karine A. Gibbs,[1] Daniel D. Isaac,[2] Jun Xu,[3†] Roger W. Hendrix,[3] Thomas J. Silhavy[2] and Julie A. Theriot[1,4*]

[1]*Department of Microbiology and Immunology, Stanford University School of Medicine, Stanford, CA 94305, USA.*
[2]*Department of Molecular Biology, Princeton University, Princeton, NJ 08544, USA.*
[3]*Pittsburgh Bacteriophage Institute and Department of Biological Sciences, University of Pittsburgh, Pittsburgh, PA 15260, USA.*
[4]*Department of Biochemistry, Stanford University School of Medicine, Stanford, CA 94305, USA.*

Summary

Advanced techniques for observing protein localization in live bacteria show that the distributions are dynamic. For technical reasons, most such techniques have not been applied to outer membrane proteins in Gram-negative bacteria. We have developed two novel live-cell imaging techniques to observe the surface distribution of LamB, an abundant integral outer membrane protein in *Escherichia coli* responsible for maltose uptake and for attachment of bacteriophage lambda. Using fluorescently labelled bacteriophage lambda tails, we quantitatively described the spatial distribution and dynamic movement of LamB in the outer membrane. LamB accumulated in spiral patterns. The distribution depended on cell length and changed rapidly. The majority of the protein diffused along spirals extending across the cell body. Tracking single particles, we found that there are two populations of LamB – one shows very restricted diffusion and the other shows greater mobility. The presence of two populations recalls the partitioning of eukaryotic membrane proteins between 'mobile' and 'immobile' populations. In this study, we have demonstrated that LamB moves along the bacterial surface and that these movements are restricted by an underlying dynamic spiral pattern.

Accepted 1 June, 2004. *For correspondence. E-mail theriot@stanford.edu; Tel. (+1) 650 725 7968; Fax (+1) 650 723 6783. †Present address: Miami Valley Laboratories, The Proctor and Gamble Company, Cincinnati, OH 45252, USA.

Introduction

Over the past decade, advances in techniques for measuring protein localization in bacteria have revealed that proteins involved in cell division and cell shape (e.g. FtsZ and MreB), virulence proteins (e.g. IcsA), chemoreceptors and flagella all have specific cellular distributions (Goldberg *et al*., 1993; Maddock and Shapiro, 1993; Steinhauer *et al*., 1999; Lybarger and Maddock, 2000; 2001; Fu *et al*., 2001; Robbins *et al*., 2001; Shapiro *et al*., 2002). Not restricted to one bacterial phylum, non-uniform subcellular localization reflects the complexity of the bacterial cell (Lybarger and Maddock, 2001). With an emphasis on cytoplasmic and inner membrane components, recent live-cell imaging using green fluorescent protein (GFP) and its derivatives (Feilmeier *et al*., 2000; Southward and Surette, 2002) has shown that these subcellular protein patterns can vary from indistinct compact accumulations to elegant helical structures and that they can change rapidly. With the advancement of deconvolution microscopy, the resolution of subcellular distributions has increased, revealing that a number of the 'indistinct accumulations', such as MinCDE in *Escherichia coli* and *Bacillus subtilis*, are in fact helices (Marston and Errington, 1999; Shih *et al*., 2003). Most prominent of these helices in Gram-negative bacteria are structures containing MreB, SetB, and the complement of Min proteins, MinCDE (Espeli *et al*., 2003; Shih *et al*., 2003), all of which are crucial for cell shape and division (Jones *et al*., 2001; Shih *et al*., 2003). GFP, however, does not fold properly for fluorescence when exported from the cytoplasm via the general secretory pathway, therefore prohibiting its use for localizing outer membrane components (Feilmeier *et al*., 2000).

While the field of bacterial cell biology is beginning to reveal the dynamic architecture inside bacteria, we still have little insight into the dynamics of the Gram-negative bacterial outer membrane surface in live cells. The overall architecture of the outer membrane, proteins interspersed with phospholipids and lipopolysaccharides (LPS), has been biochemically detailed with respect to composition ratios, fluidity and asymmetry of the inner versus outer leaflet (Jaffe and D'Ari, 1985; Souzu, 1986; Rodriguez-Torres *et al*., 1993). However, the spatial distribution of membrane components, specifically proteins, along the

surface has been elusive. A few macromolecular complexes, such as flagella and pili, are readily observed anchored peritrichously along the bacterial surface in *E. coli*, or exclusively at one pole in other Gram-negative organisms (e.g. *Pseudomonas aeruginosa* and *Vibrio cholerae*) (McCarter, 2001; Mattick, 2002; Shapiro *et al*., 2002). These organelles differ from other outer membrane structures in that they are anchored through the cell body to both periplasmic and plasma membrane components, similar to the type II and type III secretion systems (Thanassi and Hultgren, 2000).

IcsA (VirG) in *Shigella flexneri* is one of the few outer membrane proteins in Gram-negative Enterobacteriaceae whose spatial localization has been determined. A virulence protein that promotes actin polymerization, IcsA is secreted at one pole of *S. flexneri* and diffuses laterally across the cell body (Goldberg *et al*., 1993; Goldberg and Theriot, 1995; Steinhauer *et al*., 1999; Charles *et al*., 2001; Robbins *et al*., 2001). In predivisional cells, IcsA localizes asymmetrically to both cell poles, but is not found in the middle of the cell (Goldberg *et al*., 1993; Robbins *et al*., 2001). Unlike the flagella and pili components, IcsA is believed to have no periplasmic or intracellular binding partners and is integrated fully into the outer membrane as a beta-barrel. Localization of IcsA raises the question of whether other outer membrane proteins on the surface of Gram-negative bacteria might be localized to the poles. To address this, we sought to understand the dynamics and localization of the nutrient uptake protein, LamB.

LamB (maltoporin) is an abundant integral outer membrane porin, responsible for maltose uptake. Found in many species of Gram-negative bacteria, it is also the receptor for bacteriophage lambda (Randall-Hazelbauer and Schwartz, 1973; Boos and Shuman, 1998). It has been studied for the past 40 years, and its structure, function and regulation are understood on both the genetic and molecular levels. The synthesis of LamB is controlled by carbon metabolism and increases in the presence of maltose and just before division (Vos-Scheperkeuter *et al*., 1984; Boos and Shuman, 1998). LamB accepts many insertions without loss of activity, thus allowing for a wide range of epitope tags (Boulain *et al*., 1986; Newton *et al*., 1996; Andersen *et al*., 1999; Etz *et al*., 2001). Found mainly as a trimer in the outer membrane, there are $\approx$ 30 000 copies of LamB monomer present on the bacterial surface at the height of induction (Neidhardt *et al*., 1987). Early descriptions of LamB located it at the poles and septum when *E. coli* K12 cells were probed with live bacteriophage lambda, and localization depended on bacterial cell length. This led the authors to propose that LamB insertion in the outer membrane occurs at the septum in a subset of predivisional cells (Ryter *et al*., 1975). Other groups, using *lamB* on a high-copy plasmid under external (*lac* promoter) control, used indirect immunogold electron microscopy (with a primary antibody to LamB and a protein A-gold probe) to localize LamB. They demonstrated that LamB insertion into the *E. coli* K12 outer membrane occurred randomly across the entire cell body and that there was no apparent preferential insertion of LamB either at the poles or at midcell in predivisional cells (Vos-Scheperkeuter *et al*., 1984; Jaffe and D'Ari, 1985). While these studies both indicated the presence of LamB across the cell surface in fixed cells, they disagreed in their description of LamB surface localization, possibly due to the difference in detection methods or bacterial strains. Ascertaining the distribution of LamB in live cells might resolve this conflict.

By combining multiple techniques, we aim to describe the dynamics and steady-state pattern of LamB in the bacterial outer membrane. Here we have developed two novel probes for the detection of LamB in live bacterial cells. Furthermore, we have demonstrated that LamB moves dynamically in the outer membrane and that this distribution can occur along a spiral path.

Results

Fluorescently labelled bacteriophage lambda tails bind LamB on live cells

Imaging of outer membrane protein dynamics requires a probe that adheres irreversibly to cells and that can be imaged without cell fixation. We chose the tail of bacteriophage lambda as the probe for live-cell microscopy, because it is a natural ligand for LamB. We constructed a plasmid expressing only the genes required for tail self-assembly. Bacteriophage lambda tails were expressed and purified, then covalently labelled with a fluorophore, Texas Red (Fig. 1A). The resultant labelled lambda phage tail (LPT) probes were of uniform length and width as visible by transmission electron microscopy (TEM) (Fig. 1B). Striations corresponding to individual hexameric rings of the major tail subunit were quite apparent, as was the short fibre at the tip (J fibre), which directly binds LamB (Wang *et al*., 1998).

To confirm specific adherence of LPT to LamB, mid-logarithmic *E. coli* K12 were incubated with the LPT probes, washed, stained with uranyl acetate and imaged with TEM (Fig. 2). LPT visibly bound across the entire cell body of wild-type *E. coli* K12 cells (Fig. 2A). The packing density of the LPT probes was at least 40% greater than bound whole bacteriophage lambda when compared to published images (Randall-Hazelbauer and Schwartz, 1973), presumably due to a reduction in steric hindrance for the LPT probes lacking heads. Almost all LPT were exclusively bound by the tip and stood vertical to the bacterial surface (Fig. 2B). LPT were still present on the bacterial surface after centrifugation and multiple washes,

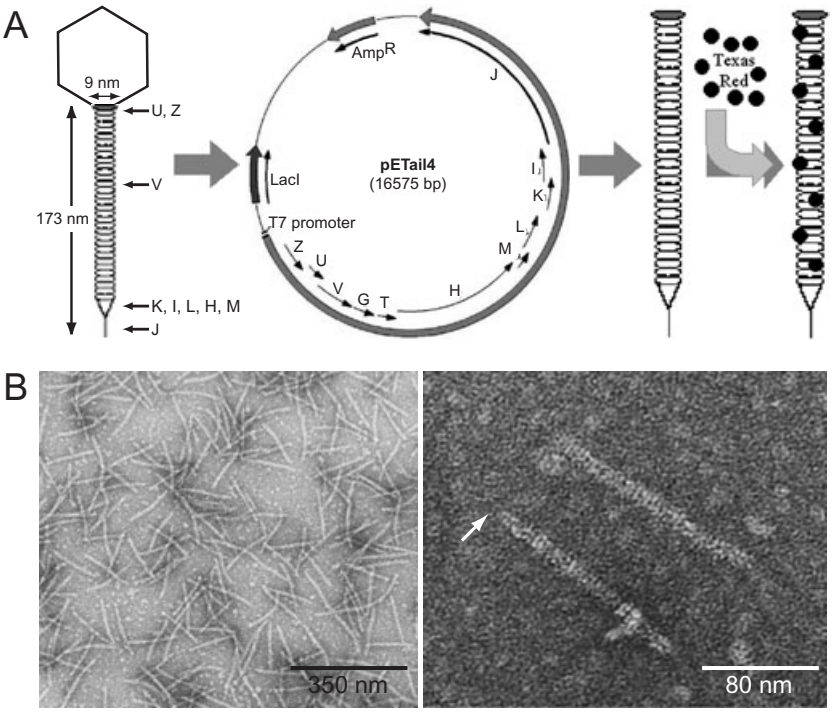

Fig. 1. Live-cell method developed for fluorescent detection of LamB using lambda phage tails (LPT).
A. Bacteriophage lambda tails were expressed from a low copy plasmid in *E. coli*, purified and covalently labelled with a fluorophore, Texas Red.
B. Negative stain electron micrographs (EM) of the labelled LPT probes. The individual hexameric rings were visible within the long tail stretch by EM, as well as the tip J fibre (marked by the arrow).

demonstrating that they bind tightly to their substrate as previously described (Weigle, 1968; Schwartz, 1976). LPT binding did not visibly affect bacterial cell morphology when compared to unlabelled wild-type cells (Fig. 2A and C). LPT did not bind to S2188, a *lamB* deletion strain (Brown, 1997), even when incubated with a fivefold greater quantity of LPT than used on wild type (Fig. 2D). These LPT probes were further used for fluorescence imaging to determine LamB surface distribution in live cells.

Spiral patterns of LamB distribution visible in live cells

To observe directly the LamB distribution *in vivo*, live-cell imaging was used. Mid-logarithmic *E. coli* K12 were incubated with Texas Red-labelled LPT probes, washed, resuspended in rich media and viewed with epifluorescence microscopy. Fluorescence from LPT was not uniform along the cell body (Fig. 3). In a population of 95 cells, two patterns were readily visible – bipolar and spiral. The remaining cells exhibited either irregular spiral or unclassifiable (other) patterns. All four observed patterns were tabulated (Table 1). No cells were observed to have a uniform distribution. Within the spiral population, many cells had an 'S' distribution in which there was a broad band of fluorescence across the middle of the cell with small unequal amounts at each pole. Longer non-dividing cells (i.e. no visible septum) had this 'S' fluorescence pattern, in which there was only one full turn of the 'S' from one end of the cell to the other (Fig. 3A, cell S). The pitch was half the length of the cell. Occasionally these cells had a 'figure 8' fluorescence in which the 'S' pattern was well defined, but the remaining edges had a very faint fluorescence. Other spiral cells exhibited a pattern with four diagonal bands in a striped pattern along the cell length. This pattern was reminiscent of the reported MreB spirals (Jones *et al*., 2001; Shih *et al*., 2003), although the pitch appears to be substantially longer for LamB than for MreB, resulting in fewer turns per cell. In total, 39% of the population exhibited a spiral pattern (Table 1).

Irregular spirals, in which the fluorescence was spiral over a portion of the cell body, but not the entire length, were also observed in long non-dividing cells (Fig. 3A, cell I). This suggested that spiral and irregular spiral populations might interconvert (see below, Fig. 4). Cells in which no consistent pattern to the fluorescence was apparent were classified as 'other', and in general, these were medium-sized cells (Fig. 3A, cell O). Shorter cells had a 'C' pattern of bipolar fluorescence in which one pole was brighter than the other with a small lateral band of fluorescence joining the two poles (Fig. 3A, cell B). This 'C' pattern appeared to be an 'S' pattern that had been split in half, perhaps because of cell division. There was no consistent pattern across all dividing cells (i.e. those with a visible septum), but there were only five within the archived population. As the LamB patterns were related to cell length, the bacterial cell cycle may affect its localization (Table 1).

Compared with traditional indirect immunofluorescence, our live-cell imaging has revealed previously unseen com-

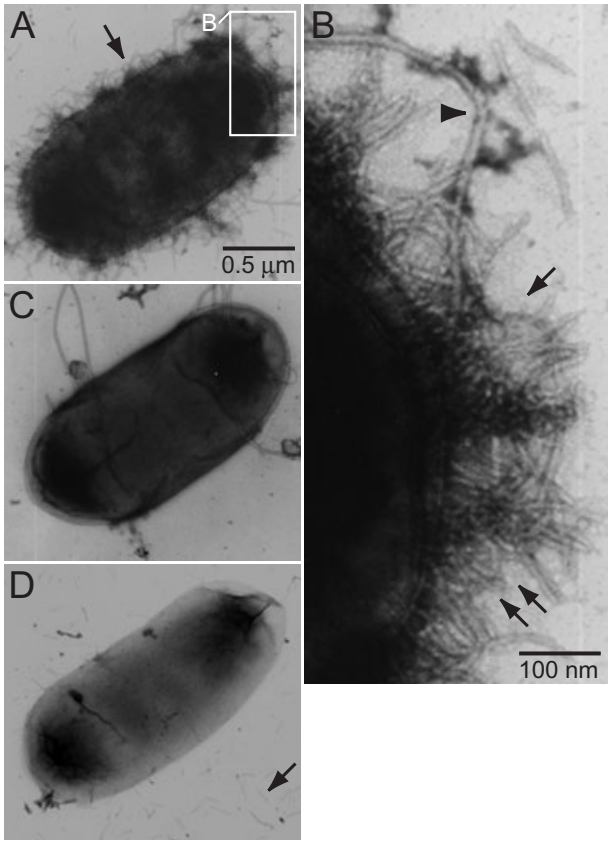

Fig. 2. LPT binding to the *E. coli* K12 surface.
A. Wild-type *E. coli* K12 cells incubated with LPT (marked by the arrow).
B. Higher magnification image of boxed region shown in A. LPT (marked by arrows) bound by the tip and stood vertical to the bacterial surface. An arrowhead indicates the flagellum.
C. *E. coli* K12 incubated without LPT.
D. S2188, a *lamB* deletion strain, incubated with a fivefold excess of LPT relative to wild-type cells. The arrow indicates unbound LPT visible in the background.

plexity in the distribution of LamB. Furthermore, our localization patterns differ from both published results of uniform and septal distributions (Ryter *et al*., 1975; Vos-Scheperkeuter *et al*., 1984). We compared our live-cell imaging with indirect immunofluorescence and the published electron microscopy images, both techniques that image dead cells. Indirect immunofluorescence was performed on mid-logarithmic *E. coli* and *S. flexneri* cells using anti-LamB antibody and a secondary antibody conjugated to the fluorophore, Texas Red (see *Supplementary material*). In the fixed cells, the fluorescence was enriched at the septum and poles, and the enrichment was much more dramatic for *S. flexneri* than for *E. coli* using the same antibody and the same technique. Thus, the previous discrepancy in the literature may have resulted from strain differences. Uneven and spiral fluorescence, which were readily visible in the live-cell imaging, were not observed on the fixed cells (see quantitative analysis in *Supplemental material*). Comparison of these results with our live-cell images suggests that either cell fixation or amplification by secondary antibodies in immunofluorescence causes mislocalization or extraction of LamB from the outer membrane, as has previously been observed in eukaryotic cells (Palade, 1952; Sabatini *et al*., 1963). Additionally, antibody recognition is sometimes obscured by occlusion of antigenic sites by LPS or other components, especially when the antigenic site is not externally accessible (Voorhout *et al*., 1986). The static images of live LamB localization suggested a range of steady-state distributions; next we wished to observe transitions among these patterns in real time.

LamB moves rapidly in the outer membrane

The dynamics of LamB movement in the outer membrane was observed using time-lapse microscopy of LPT-labelled live cells. Images were taken every 20 s for 5 min (Fig. 4A; Fig. S1). Averaging over all images taken within one movie gave an 'S' spiral pattern observed in some still images, although some individual frames contained higher-order or irregular spirals (Fig. 4A and B). Within this 5 min movie, major shifts in the observed fluorescence pattern occurred between 40 and 60 s, between 80 and 100 s and between 200 and 220 s. Also, this cell showed spiral (100–180 s) and irregular spiral (220–260 s) distributions. This suggested that on average the arrangement of LamB in a mid-sized cell is a one-turn spiral that is dynamically composed of transient more

Table 1. Length of cells in observed patterns.

Class	*n*	% of population	Mean length (μm)	95% CI (μm)	Outlines of LamB in representative cells
Bipolar	16	17	2.03	1.89–2.16	
Spiral	37	39	2.60	2.43–2.78	
Irregular spirals	25	26	2.62	2.46–2.78	
Other	17	18	2.18	2.00–2.35	
Total (population)	95	100	2.44	2.34–2.54	

CI, confidence interval.

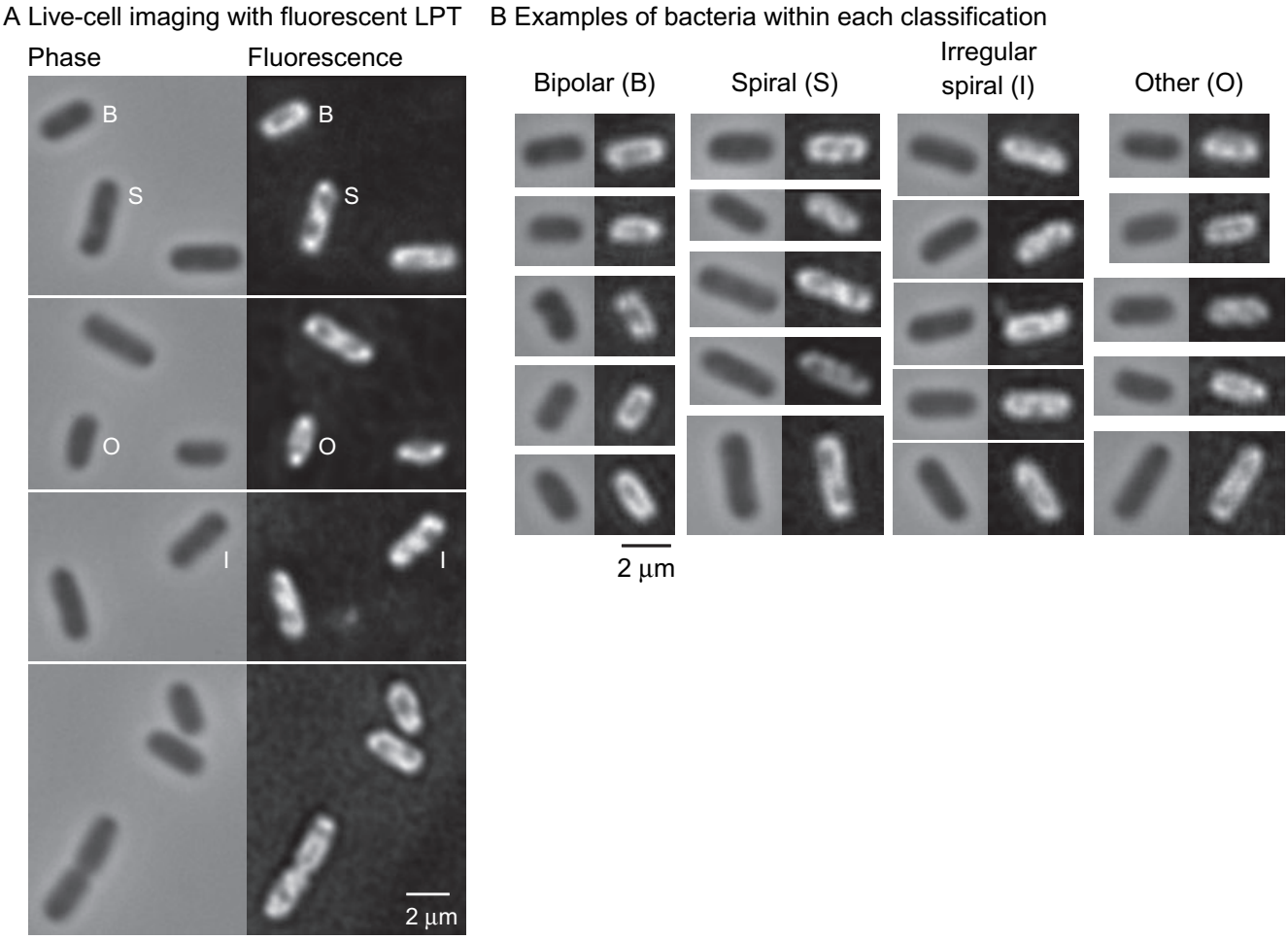

Fig. 3. Direct epifluorescence microscopy with fluorophore-labelled LPT.
A. Mid-logarithmic *E. coli* K12 cells were incubated with LPT and imaged live with epifluorescence microscopy. Cell B, bipolar; cell S, spiral; cell I, irregular spiral; cell O, other. (Phase images, left; fluorescence images, right).
B. Representative images of individuals within each classification are presented. None of these individuals are presented in (A). The diversity and similarity between classes was readily apparent. (Phase images, left; fluorescence images, right).

complex tightly wound irregular spirals. Changes were detected every 20 s, indicating that LamB moved rapidly along the surface. Only 3–11% of the protein population moved during a 20 s interval, as measured by the normalized change in fluorescence distribution. Changes over a 20 s interval were similar for all regions of the cell. Over the course of the movie, the normalized fluorescence at the midcell increased slightly, suggesting a preferential accumulation of LamB. The poles correlated with each other in fluorescence intensities for the duration of the movie and were anti-correlated to the changes at midcell. This implied a dynamic balance between proteins located at the poles and at the middle. Protein diffusion within the remainder of the cell appeared to be independent of location. From these results, individual LamB proteins may move large distances reminiscent of compression waves. Alternatively, subsets of LamB proteins may move while other subsets remain stationary. Fluorescent labelling of the whole population with LPT cannot distinguish between these possibilities; we therefore needed to devise a technique to follow the motion of single LamB particles.

Tracking individual LamB monomers with colloidal gold

A gold-binding epitope (Brown *et al.*, 2000) was inserted into loop 4 (between amino acids 155 and 156) of LamB under the *lac* promoter to enable labelling and tracking of individual LamB proteins. *E. coli* K12 cells were incubated with ≈ 20 nm colloidal gold, washed, resuspended in LB and imaged. The colloidal gold readily bound the bacterial surface when the epitope-tagged LamB was present (Fig. 5A, IPTG+). Colloidal gold did not bind uninduced (IPTG–) cells or cells lacking the insertion. Diffraction of transmitted light by the gold particles renders their images

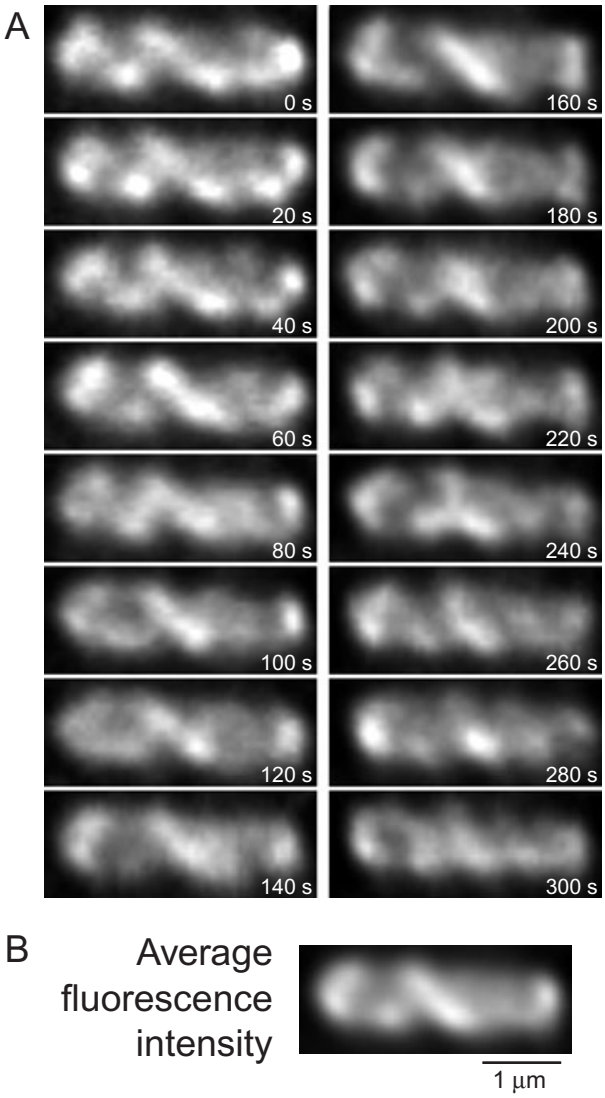

Fig. 4. Time-lapse direct epifluorescence microscopy with LPT.
A. Images of this LPT-labelled cell were taken every 20 s for 5 min. At various time points, this cell showed spiral (100–180 s) and irregular spiral (220–260 s) distributions.
B. The fluorescence intensity of all images taken within this movie (A) were normalized and averaged.

substantially larger than the true particle size, and enables centroid tracking of the 20 nm particles using light microscopy. Time-lapse images were taken of colloidal gold-bound cells (1 s intervals over 5 min). Semi-automated centroid tracking of the gold particles revealed that the gold diffused differentially in nanometer steps.

When all LamB monomers contained the gold-binding epitope (strain DDI100), two populations of LamB proteins were observed: slow-moving and fast-moving. The slow-moving population moved ≈ 20–50 nm in 5 min, while the fast-moving population moved up to 300 nm in 5 min (Fig. 5B). To address the possibility that the slow-moving population might represent gold simultaneously bound to multiple LamB trimers, we repeated these experiments with the epitope-tagged LamB expressed in the presence of wild-type LamB (strain DDI101). The number of fast- and slow-moving particles was comparable in both strains (DDI100: nine fast, 11 slow; DDI101: seven fast, 11 slow), indicating that the slow- and fast-moving gold particles more likely represent individual LamB proteins with intrinsically different mobility. We also looked at a lower induction of epitope-tagged LamB (0.01 mM IPTG) in strain DDI101 under the same experimental conditions. We observed the presence of two populations (three fast, eight slow), and these populations displayed equivalent behaviour to the populations observed at the higher IPTG (1 mM) induction. Both the fast- and slow-moving populations had diffusion kinetics consistent with bounded diffusion (Fig. 5C). In bounded diffusion, indicated by the horizontal asymptote in the mean-squared displacement (MSD) plotted over sequential time intervals, a particle does not move randomly or freely through a fluid; for free, unbounded diffusion, the plot of MSD versus time would show a constant linear increase. This suggested that the slow-moving LamB (≈ 60% of the population) might be more tightly bound to the peptidoglycan layer or some other cellular component. The restricted motion of the slow population, however, is not sufficient to explain the large-scale movements we observed when using the labelled lambda tails (Fig. 4).

The fast-moving (40%) population, however, diffused more freely, moving between 100 and 300 nm in 5 min, which is consistent with the changes we observed with the fluorescent LPT (Fig. 5B). The gold particles within the fast-moving population diffused a larger distance over small (5 s) intervals than those within the slow-moving population, demonstrating that the fast-moving population was usually diffusing larger distances than the slow-moving population. This indicates a persistent underlying difference in the anchoring of the two populations. There was no apparent correlation between fast versus slow movement and location on the bacterial surface, suggesting that there was no preferred domain for faster- or slower-moving LamB protein. These subpopulations of LamB were present across the bacterial surface, suggesting that both the fast- and slow-moving populations coexist within the observed spiral patterns. While mobile and immobile subpopulations of membrane proteins have been described for eukaryotic cells, this is one of the first examples observed in the bacterial membrane.

Discussion

We have demonstrated that LamB, an integral outer membrane protein involved in nutrient uptake, is non-uniformly distributed on the surface of *E. coli* and that the distribution of this protein changes within tens of seconds (Fig. 4).

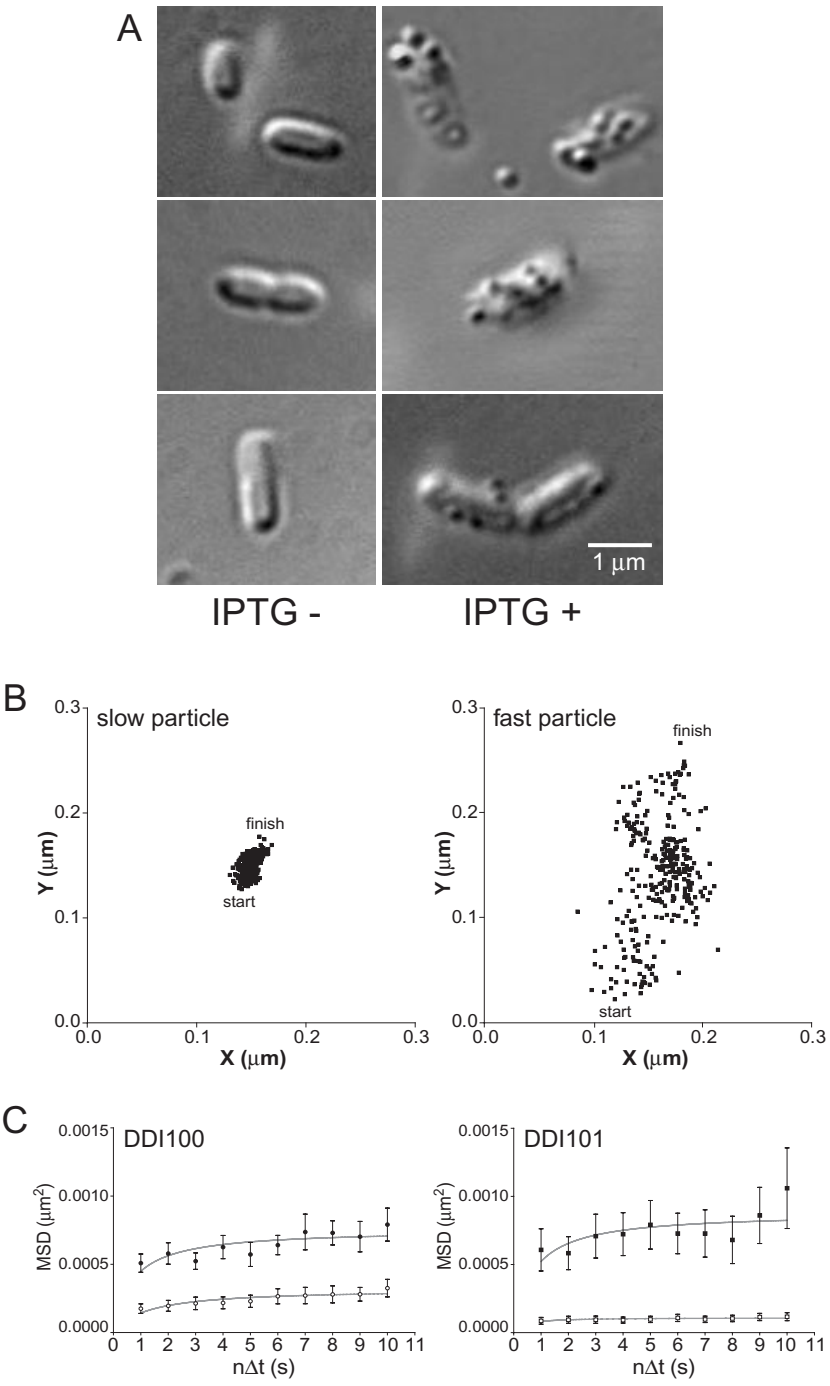

Fig. 5. Single-particle tracking of gold-bound LamB protein.
A. DIC images of uninduced (IPTG–) and induced (IPTG+) *E. coli* K12 cells incubated with ≈ 20 nm colloidal gold. These cells express an IPTG-inducible LamB protein encoding a gold-binding epitope.
B. The motion of colloidal gold was followed over 5 min at 1 s intervals using semi-automated tracking. Two populations were observed – slow and fast. The slow particles moved very short distances (20–50 nm), while the fast particles diffused much greater distances (100–300 nm). Presented are two representative tracks from the DDI100 population.
C. Diffusion of colloidal gold-bound LamB in both the absence (DDI100) and presence (DDI101) of wild-type LamB. *E. coli* cells were visualized by DIC microscopy with frames recorded every second for 5 min. The centre of 38 total gold particles (DDI100: 20, DDI101: 18) was tracked. The mean-squared displacement (MSD) was calculated from the X, Y positions of colloidal gold and plotted as a function of time ($n\Delta t$). Slight differences between DDI100 and DDI101 are not statistically significant. Error bars are standard error of the mean. Fast, closed symbols; slow, open symbols.

To follow protein movement in the membrane, we developed two live-cell microscopy techniques – one using tails from bacteriophage lambda, which bind to LamB to initiate phage infection, and the other using colloidal gold bound to an epitope tag on the LamB protein itself. We have also shown that indirect immunofluorescence does not provide a fully accurate description of LamB distribution in the outer membrane. Chemical fixation of the fluid outer membrane in bacteria appears to extract proteins, as has been previously described in eukaryotic cells (Palade, 1952; Sabatini *et al.*, 1963). Thus, imaging without fixation is crucial for retaining the native distributions of surface proteins and requiring the use of non-invasive live-cell techniques.

The majority of the bacterial population labelled with LPT displayed a spiral pattern of fluorescence, while the rest mainly had irregular spiral or bipolar distributions, and none had uniform distributions. While we observed an

accumulation at midcell, LamB was also spread across the entire cell length. Time-lapse microscopy indicated that these LamB spirals are dynamic, in that a subset (3–11%) of the protein redistributes along the cell length every 20 s. This is comparable to reported cytoplasmic mobility for MinCDE in *E. coli*, in which protein oscillated from one pole to the other in ≈ 20 s (Hu and Lutkenhaus, 1999; Raskin and de Boer, 1999a,b). For the Min system, the protein movement is based on polymerization and depolymerization of apparently colocalized spirals. There appears to be a portion of the Min proteins that does not depolymerize, which may provide a permanent scaffold on which subsequent polymerization can occur (Gitai and Shapiro, 2003; Shih *et al*., 2003). Similarly, we observed two populations of LamB – mobile and immobile. The spiral distribution of LamB does not follow the dynamics of a fixed spiral like Mbl in *B. subtilis*. Helices of Mbl, a bacterial actin homologue, remain stationary, but the components are continuously recycled (Carballido-Lopez and Errington, 2003). In contrast, FtsZ in sporulating *B. subtilis* migrates to the pole through helical intermediates, resulting in a conformational change of the large population between tightly and loosely compacted helices (Ben-Yehuda and Losick, 2002). This dynamic migration of FtsZ polymer is more similar to the motion we observe in the LamB population. As both the mobile and immobile protein populations are distributed throughout the spiral pattern, it is possible that the immobile proteins provide a 'path' upon which the mobile LamB protein can move. This suggests that there may be relatively tight protein–protein interactions on the cell surface. Alternatively, the LamB population may be excluded from the rest of the cell surface due to spatially restricted accumulations of lipids, LPS, or other proteins.

Recent work has shown that some lipids in the inner membrane of Gram-negative bacteria separate into subdomains. Cardiolipin is observed dispersed along the inner membrane at apparently regular intervals and especially near the poles and midcell (Mileykovskaya and Dowhan, 2000). Also, the separation into distinct membrane domains by two fluorescently labelled phospholipids, 2-pyrene-decanoyl-phosphatidylethanolamine and 2-pyrene-decanoyl-phosphatidylglycerol, is seen in the inner membrane of *E. coli* and the cell membrane of *B. subtilis* (Vanounou *et al*. 2003). The presence of lipid subdomains in the inner membrane raises the possibility of similar phase separation in the outer membrane. The outer leaflet of the outer membrane is almost exclusively composed of LPS, while phospholipids mostly comprise the inner leaflet (Nikaido, 2003). Strong lateral interactions between LPS molecules may contribute to the low permeability of the outer membrane (Nikaido, 2003). Similar lateral interactions have been observed with glycosphingolipids in eukaryotic cell membranes; glycosphingolipids form 'rafts' in the membrane and the presence of these result in decreased membrane permeability (Hill and Zeidel, 2000; London and Brown, 2000). LPS, like glycosphingolipids, may form stable domains in the outer membrane due to the tight interactions among neighbouring molecules (Nikaido, 2003). These strong interactions of LPS molecules may also induce patches of LPS (i.e. rafts) in which protein is excluded from LPS domains in the outer membrane. This, however, still fails to address whether the observed LamB structure results from exclusion by lipids or by other proteins. Colocalization studies with other outer membrane components might discern the exclusivity of the LamB pattern. LamB was uninduced in our studies. Observing the LamB distribution after induction or under repressed conditions may lead to a change in distribution pattern as well as a change in the mobility of LamB in the outer membrane.

The presence of two separate populations of LamB within the outer membrane is similar to observations of protein behaviour in eukaryotic cell membranes. Between 30% and 90% of integral membrane proteins, such as asialoglycoproteins, are mobile in the eukaryotic plasma membrane, with the remaining fraction anchored to some cellular component, presumably the cytoskeleton (Henis *et al*., 1990). Here we observed by single-particle tracking that ≈ 40% of the LamB population in the outer membrane is mobile. The mobile LamB population moved up to 300 nm in 5 min, suggesting that these proteins are not as tightly bound to subcellular structures as the immobile subpopulation. Moreover, the lipid (phospholipid and LPS) composition in the outer membrane does not prohibit lateral diffusion (Sandlin *et al*., 1995; Robbins *et al*., 2001). For single-particle tracking experiments, we used a probe with a diameter of ≈ 20 nm in this study, compared to probes with a diameter of ≈ 500 nm used in other studies (Oddershede *et al*., 2002). The use of even smaller probes may show that the fast LamB population is indeed more mobile. The immobile LamB population was restricted to a region of 50 nm over 5 min, which is consistent with previously published single-particle tracking of LamB using optical tweezers (Oddershede *et al*., 2002).

The restraint on this subpopulation may result from many factors, including anchoring to the peptidoglycan layer or association with a periplasmic factor. Previous studies have shown that 30–40% of LamB in *E. coli* is non-covalently associated with the peptidoglycan layer (Gabay and Yasunaka, 1980). Attachment with the peptidoglycan layer may provide a mechanism for the observed spiral distribution. It has been reported that peptidoglycan in *E. coli* is synthesized ubiquitously across the bacterial length, with the exception of the old poles, at which no new peptidoglycan synthesis occurs (de Pedro *et al*., 1997). Early images from de Pedro *et al*. (1997) suggest peptidoglycan incorporation in a helical pattern in *E. coli*,

but data on this remains sparse. However, in Gram-positive bacteria, helical incorporation of peptidoglycan into the cell wall has been readily observed, possibly because of the much larger thickness of the Gram-positive cell wall (Mendelson, 1976; Wolfe and Mendelson, 1987; Surana *et al*., 1988; Daniel *et al*., 2000; Scheffers *et al*., 2004). If a subset of LamB is bound to the peptidoglycan, even transiently, this may orient the protein population to maintain the same structure as the underlying synthesized wall.

Here we have demonstrated that at least one integral outer membrane protein has dynamic spiral localization. This protein, LamB, exists as two populations (mobile and immobile) within the outer membrane, which has yet to be observed with other integral outer membrane proteins. The fast diffusion of the mobile subpopulation is responsible for rapid changes to the large-scale spiral distribution pattern of LamB. Through these studies, we have just begun to uncover the dynamic topography of the bacterial outer membrane. With the development of novel live-cell techniques, the properties of this once poorly described surface will be elucidated and incorporated into our growing insight into the cell biology of bacteria.

Experimental procedures

Bacterial strains and growth conditions

The bacterial strains and plasmids used in this study are listed in Table 2. *E. coli* and *S. flexneri* strains were grown to mid-logarithmic phase in Luria–Bertani (LB) broth and tryptic soy broth respectively (Miller, 1992). Antibiotics were used, when appropriate, at the following concentrations: chloramphenicol, 35 μg ml^{-1}, carbenicillin, 100 μg ml^{-1}.

Construction of pETail4, the plasmid expressing tail proteins of bacteriophage lambda

A 16 kb *Bam*HI-*Eco*RI fragment of λ DNA containing all 11 tail genes was cloned into the *Bam*HI and *Eco*RI sites of pBluescript SK– (Stratagene) to create pBS-λ-tail-I. The large fragment from a *Bsi*WI-*Hind*II digestion of pBS-λ-tail-I was filled in and circularized to create pBS-λ-tail3. pBS-λ-tail3 was cut with *Bam*HI, filled in and then cut with *Nsi*I and ligated to a 2.6 kb *Bsa*AI-*Nsi*I fragment of pBS-λ-tail-I to create pBStail5. The *Sac*I-*Xho*I fragment of pBStail5 was inserted between the *Sac*I and *Xho*I sites of pET21+ (Novagen) to create pETail-I. A *Bst*BI-*Xho*I digestion of a polymerase chain reaction (PCR) fragment produced by using primers J1 (5'-GAGGAGTTTTCGAAAG-3'), J2 (5'-GGCTCGAGACGAACCTCTGTAAC-3') and pETail-I as template was inserted back into the *Bst*BI-*Xho*I sites of pETail-I. The resulting construct, pETail4, lacks the *lom* gene and has about 20 bp downstream of gene *J*.

Purification and fluorophore-labelling of lambda phage tails (LPT)

Escherichia coli BL21(DE3)-Δtail cells harbouring pETail4 were diluted 1:100 into fresh LB media from overnight cultures. After 2 h at 37°C, they were induced with 1 mM IPTG (isopropyl-beta-D-thiogalactopyranoside) and grown until mid-logarithmic phase. Cells were harvested and lysed in lysis buffer (50 mM Tris pH 8.0 and 5 mM EDTA), 0.2% Triton X-100, 6 mM $MgSO_4$, 10 μg ml^{-1} RNAse A and 10 μg ml^{-1} DNAse I at 30°C. The cell debris was spun out, and the LPT in the supernatant were precipitated in 0.7 M 1-glutamic acid (KGlu) and 7.5% polyethylene glycol (PEG) 8000. The LPT were harvested by centrifugation and resuspended in TKG (20 mM Tris-HCl, pH 7.5 and 100 mM KGlu). They were then purified in TKG over a 5% step gradient of glycerol (10–30%). The LPT were recovered from the 15% gradient step and pelleted. The LPT pellet was resuspended in 0.1 M $NaHCO_3$ and dialysed overnight at 4°C in the same buffer. LPT were labelled with a 5000-fold molar excess of Texas Red-sulphonyl chloride (TR) using the supplied protocol (Molecular Probes). TR-labelled LPT were dialysed against 0.1 M $NaHCO_3$ overnight at 4°C and then separated from free dye by gel filtration over a Nap-5 column in 0.1 M $NaHCO_3$ using the supplied protocol (Amersham Biosciences). The fractions containing TR-labelled LPT were pooled for use. The purity of LPT was confirmed by 12.5% SDS-PAGE and TEM (by negative stain). Probes were stable for 30 days when stored at 4°C.

Table 2. List of strains and plasmids.

Strain	Relevant genetic markers or features	Reference or source
Escherichia coli		
MG1655	F$^-$ lambda- *ilvG$^-$ rfb-50 rph-1*	Blattner *et al.* (1997)
S2188	F$^-$ *lacI^Q ΔlamB106 endA hsdR17 supE44 thi1 relA1 gyrA96 ΔfimB-H::kan*	Brown (1997)
DDI100	S2188 pDDI2	This study
DDI101	S2188 *lamB$^+$* pDDI2	This study
BL21(DE3)-Δtail	F$^-$ *ompT gal [dcm] [lon] hsdSB*(rB$^-$ mB$^-$; an *E. coli* B strain) with DE3 (Studier *et al*., 1990) (with the tail portion of DE3 knocked out)	This study
Plasmids		
pDDI2	*lamB* with RP6 (Brown *et al*., 2000) inserted between codons 155 and 156 in pSB2267 (Brown, 1997)	This study
pETail4	λ ZUVGTHMLKIJ in pET21$^+$	This study
pSB2267	LamB expression vector with *Eco*RI and *Eco*RI-*Stu*I fragments of pAC1 in the *Cla*I-*Bcl*I fragment of pACYC184	Brown (1997)

Transmission electron microscopy

Escherichia coli cells were grown from overnight inoculates (1:100 dilution) to mid-logarithmic in LB at 37°C. The bacterial cells were washed twice with phosphate-buffered saline (PBS) (1 mM $CaCl_2$, 2.7 mM KCl, 2 mM KH_2PO_4, 0.5 mM $MgCl_2$, 137 mM NaCl and 10 mM Na_2HPO_4) and resuspended in LB. Cells were then incubated with purified LPT at room temperature, shaking for 20 min. Unbound LPT were removed from the reaction mixture by a wash with PBS. The washed cells were resuspended in PBS and used for TEM. Carbon-coated grids were floated in 20 μl of sample for 2 min to allow bacteria to bind the grid. The grids were then washed twice in PBS and stained for 2 min in uranyl acetate. The grids were scanned and imaged on a Phillips CM 12 transmission electron microscope.

Transmitted light and epifluorescence live-cell microscopy

Cells incubated with LPT were prepared as described above for TEM, except after incubation with labelled LPT, they were washed once with PBS and resuspended in LB. Cells were then mounted in a small drop (2 μl) of LB between a slide and coverslip with 1 μm latex spacer beads, and sealed with VALAP (vaseline:lanolin:paraffin, 1:1:1). The cells were maintained at room temperature for the duration of labelling and imaging. Images were captured on an Axioplan 2 microscope equipped with phase-contrast, differential interference contrast (DIC) and epifluorescence optics (Carl Zeiss) and a back-thinned cooled charge-coupled device camera (MicroMAX 512 BFT; Princeton Instruments). LamB localization was observed using a 100× N.A. 1.4 objective lens coupled with a 2×-magnifying lens in front of the camera. Sixteen-bit images were captured using MetaMorph software (Universal Imaging). Out-of-focus fluorescence was removed from attained images using 2D Blind Deconvolution in the AutoQuant AutoDeblur software package (AutoQuant Imaging, Inc.). Images were then converted to eight-bit images in Image J (National Institutes of Health) and Adobe Photoshop (Adobe Systems). Using these images, cells were classified into 'bipolar', 'spiral', 'irregular spiral' and 'other' groupings by three independent observers.

Indirect immunofluorescence

Escherichia coli and *S. flexneri* cells were grown from overnight inoculates (1:100 dilution) to mid-logarithmic phase in appropriate media at 37°C. The bacterial cells were washed with PBS, mounted on glass coverslips and fixed for 15 min in 3.7% formaldehyde in PBS. Indirect antibody labelling of the cells was performed as described (Robbins *et al*., 2001). In brief, the cells on coverslips were first incubated with anti-LamB antibody (Bowers *et al*., 2003) in block solution (PBS with 0.2% bovine serum albumin) for 1 h and washed with PBS. They were then incubated with a secondary goat anti-rabbit antibody conjugated to Texas Red (Jackson ImmunoResearch Laboratories) in block solution for 30 min and washed with PBS. Coverslips were mounted on slides with anti-fade and sealed with clear nail polish. Microscopy was performed as described above for live cells.

Construction of LamB derivatives with gold-epitope inserts

The gold-binding insert is located between codons 155 and 156 of mature LamB that has been mutated to create a *Pst*I and *Xho*I site respectively (Brown, 1997). Plasmid pDDI2 was constructed by digesting pSB2267 with *Pst*I and *Xho*I to linearize it and cloning in the *Pst*I-*Xho*I (RP6) fragment from pSB3246, which encodes lqt(qatsGSERMGHQSGTVH PGkt)$_7$qatsle (Brown *et al*., 2000). This construct produced molecules that could form higher-order LamB structures as assayed by gentle-lysis Western blot (Rizzitello *et al*., 2001) and were shown to be functional for maltodextrin transport as assayed in a strain lacking any functional LamB (S2188) on dextrin-MacConkey agar. Strain DDI101 was constructed by transduction of *lamB*$^+$ into strain S2188 using P1 *vir* selecting for Dex$^+$ on dextrin minimal agar and transforming the resultant strain to chloramphenicol resistance with pDDI2. Presence of wild-type LamB was confirmed by Western blot.

Imaging and tracking gold-epitope LamB

Strains DDI100 and DDI101 were diluted 1:100 into the appropriate media from overnight cultures. After 2 h at 37°C, they were induced with 1 mM IPTG and grown until mid-logarithmic. The bacterial cells were washed twice with PBS and resuspended in LB. Cells were then incubated with a fivefold greater volume of ≈ 20 nm colloidal gold (Ted Pella) at room temperature, rotating for 20 min. Cells were washed once with PBS and resuspended in LB. Samples were mounted between a slide and coverslip with 1 μm latex spacer beads, and the coverslip was sealed with VALAP. Images were captured as described above and taken at 1 s intervals over 5 min.

Colloidal gold movement was followed using semi-automated centroid tracking (MetaMorph), and the diffusion constraints and coefficients were determined as described (Qian *et al*., 1991; Saxton, 1997; Giardini and Theriot, 2001; Oddershede *et al*., 2002). The centroid of each gold particle was determined for each frame in the video sequence, and stage drift was corrected by tracking spacer beads adhered to the glass coverslip. Only cells with one or two attached gold particles were tracked. The mean-squared displacement MSD($n\Delta t$) was calculated for all non-overlapping consecutive pairs of values.

Acknowledgements

We thank Dale Kaiser, Denise Monack, Patrick Viollier and Aretha Fiebig for helpful discussion and comments on the manuscript. We also thank Matthew Footer and Robert Duda for advice in developing the tail purification protocol and in adapting it for fluorescent labelling, Stanley Brown for advice about the gold-binding strains, Catherine Lacayo and Susanne Rafelski for bacterial classification, Zachary Pincus for help with analysis and Nafisa Ghori for aid with the electron microscopy. This work was supported by a Fellowship for Science and Engineering from the David and Lucile Packard Foundation to J.A.T. and by National Institutes of Health Grant AI36929 to J.A.T., NIH Grant GM34821 to T.J.S. and

NIH Grant GM47795 to R.W.H. A National Science Foundation Graduate Research Fellowship, a Stanford Graduate Fellowship and an American Society for Microbiology Robert D. Watkins Minority Graduate Research Fellowship supported K.A.G.

Supplementary material

The following material is available from
http://www.blackwellpublishing.com/products/journals/suppmat/mmi/mmi4242/mmi4242sm.htm

Fig. S1. Live *E. coli* K-12 cells with bound LPT were imaged using time-lapse direct epifluorescence microscopy. Images were taken every 20 s for 5 min. Over the course of this movie, this cell showed both spiral and irregular spiral distributions.

Fig. S2. A. Indirect immunofluorescence microscopy of LamB. B. Three major distribution patterns of LamB on the bacterial surface. C. Peak fluorescence intensity occurs at the poles and at mid-cell. D. Peak fluorescence correlates with bacterial size in *S. flexneri.*

References

Andersen, C., Bachmeyer, C., Tauber, H., Benz, R., Wang, J., Michel, V., *et al.* (1999) *In vivo* and *in vitro* studies of major surface loop deletion mutants of the *Escherichia coli K-12* maltoporin: contribution to maltose and maltooligosaccharide transport and binding. *Mol Microbiol* **32:** 851–867.

Ben-Yehuda, S., and Losick, R. (2002) Asymmetric cell division in *B. subtilis* involves a spiral-like intermediate of the cytokinetic protein FtsZ. *Cell* **109:** 257–266.

Blattner, F.R., Plunkett, G., 3rd, Bloch, C.A., Perna, N.T., Burland, V., Riley, M., *et al.* (1997) The complete genome sequence of *Escherichia coli* K-12. *Science* **277:** 1453–1474.

Boos, W., and Shuman, H. (1998) Maltose/maltodextrin system of *Escherichia coli*: transport, metabolism, and regulation. *Microbiol Mol Biol Rev* **62:** 204–229.

Boulain, J.C., Charbit, A., and Hofnung, M. (1986) Mutagenesis by random linker insertion into the *lamB* gene of *Escherichia coli* K12. *Mol Gen Genet* **205:** 339–348.

Bowers, C.W., Fau, L., and Silhavy, T.J. (2003) Secretion of LamB-LacZ by the signal recognition pathway of *Escherichia coli*. *J Bacteriol* **185:** 5697–5705.

Brown, S. (1997) Metal-recognition by repeating polypeptides. *Nature Biotechnol* **15:** 269–272.

Brown, S., Sarikaya, M., and Johnson, E. (2000) A genetic analysis of crystal growth. *J Mol Biol* **299:** 725–735.

Carballido-Lopez, R., and Errington, J. (2003) The bacterial cytoskeleton: *in vivo* dynamics of the actin-like protein Mbl of *Bacillus subtilis*. *Dev Cell* **4:** 19–28.

Charles, M., Perez, M., Kobil, J.H., and Goldberg, M.B. (2001) Polar targeting of *Shigella* virulence factor IcsA in *Enterobacteriaceae* and *Vibrio*. *Proc Natl Acad Sci USA* **98:** 9871–9876.

Daniel, R.A., Harry, E.J., and Errington, J. (2000) Role of penicillin-binding protein PBP 2B in assembly and functioning of the division machinery of *Bacillus subtilis*. *Mol Microbiol* **35:** 299–311.

Espeli, O., Nurse, P., Levine, C., Lee, C., and Marians, K.J. (2003) SetB: an integral membrane protein that affects chromosome segregation in *Escherichia coli*. *Mol Microbiol* **50:** 495–509.

Etz, H., Minh, D.B., Schellack, C., Nagy, E., and Meinke, A. (2001) Bacterial phage receptors, versatile tools for display of polypeptides on the cell surface. *J Bacteriol* **183:** 6924–6935.

Feilmeier, B.J., Iseminger, G., Schroeder, D., Webber, H., and Phillips, G.J. (2000) Green fluorescent protein functions as a reporter for protein localization in *Escherichia coli*. *J Bacteriol* **182:** 4068–4076.

Fu, X., Shih, Y.L., Zhang, Y., and Rothfield, L.I. (2001) The MinE ring required for proper placement of the division site is a mobile structure that changes its cellular location during the *Escherichia coli* division cycle. *Proc Natl Acad Sci USA* **98:** 980–985.

Gabay, J., and Yasunaka, K. (1980) Interaction of the LamB protein with the peptidoglycan layer in *Escherichia coli* K12. *Eur J Biochem* **104:** 13–18.

Giardini, P.A., and Theriot, J.A. (2001) Effects of intermediate filaments on actin-based motility of *Listeria monocytogenes*. *Biophys J* **81:** 3193–3203.

Gitai, Z., and Shapiro, L. (2003) Bacterial cell division spirals into control. *Proc Natl Acad Sci USA* **100:** 7423–7424.

Goldberg, M.B., Barzu, O., Parsot, C., and Sansonetti, P.J. (1993) Unipolar localization and ATPase activity of IcsA, a *Shigella flexneri* protein involved in intracellular movement. *Infect Agents Dis* **2:** 210–211.

Goldberg, M.B., and Theriot, J.A. (1995) *Shigella flexneri* surface protein IcsA is sufficient to direct actin-based motility. *Proc Natl Acad Sci USA* **92:** 6572–6576.

Henis, Y.I., Katzir, Z., Shia, M.A., and Lodish, H.F. (1990) Oligomeric structure of the human asialoglycoprotein receptor: nature and stoichiometry of mutual complexes containing H1 and H2 polypeptides assessed by fluorescence photobleaching recovery. *J Cell Biol* **111:** 1409–1418.

Hill, W.G., and Zeidel, M.L. (2000) Reconstituting the barrier properties of a water-tight epithelial membrane by design of leaflet-specific liposomes. *J Biol Chem* **275:** 30176–30185.

Hu, Z., and Lutkenhaus, J. (1999) Topological regulation of cell division in *Escherichia coli* involves rapid pole to pole oscillation of the division inhibitor MinC under the control of MinD and MinE. *Mol Microbiol* **34:** 82–90.

Jaffe, A., and D'Ari, R. (1985) Growth of the *Escherichia coli* cell envelope. *Biochimie* **67:** 141–144.

Jones, L.J., Carballido-Lopez, R., and Errington, J. (2001) Control of cell shape in bacteria: helical, actin-like filaments in *Bacillus subtilis*. *Cell* **104:** 913–922.

London, E., and Brown, D.A. (2000) Insolubility of lipids in Triton X-100: physical origin and relationship to sphingolipid/cholesterol membrane domains (rafts). *Biochim Biophys Acta* **1508:** 182–195.

Lybarger, S.R., and Maddock, J.R. (2000) Differences in the polar clustering of the high- and low-abundance chemoreceptors of *Escherichia coli*. *Proc Natl Acad Sci USA* **97:** 8057–8062.

Lybarger, S.R., and Maddock, J.R. (2001) Polarity in action: asymmetric protein localization in bacteria. *J Bacteriol* **183:** 3261–3267.

McCarter, L.L. (2001) Polar flagellar motility of the *Vibrionaceae*. *Microbiol Mol Biol Rev* **65:** 445–462.

Maddock, J.R., and Shapiro, L. (1993) Polar location of the chemoreceptor complex in the *Escherichia coli* cell. *Science* **259:** 1717–1723.

Marston, A.L., and Errington, J. (1999) Selection of the mid-cell division site in *Bacillus subtilis* through MinD-dependent polar localization and activation of MinC. *Mol Microbiol* **33:** 84–96.

Mattick, J.S. (2002) Type IV pili and twitching motility. *Annu Rev Microbiol* **56:** 289–314.

Mendelson, N.H. (1976) Helical growth of *Bacillus subtilis*: a new model of cell growth. *Proc Natl Acad Sci USA* **73:** 1740–1747.

Mileykovskaya, E., and Dowhan, W. (2000) Visualization of phospholipid domains in *Escherichia coli* by using the cardiolipin-specific fluorescent dye 10-N-nonyl acridine orange. *J Bacteriol* **182:** 1172–1175.

Miller, J.H. (1992) *A Short Course in Bacterial Genetics.* Cold Spring Harbor, NY: Cold Spring Harbor Laboratory Press.

Neidhardt, F.C., Ingraham, J.L., Low, K.B., Magasanik, B., Schaechter, M., and Umbarger, H.E. (1987) *Escherichia coli* and *Salmonella typhimurium*: Cellular and Molecular biology. Washington, DC: American Society for Microbiology.

Newton, S.M., Klebba, P.E., Michel, V., Hofnung, M., and Charbit, A. (1996) Topology of the membrane protein LamB by epitope tagging and a comparison with the X-ray model. *J Bacteriol* **178:** 3447–3456.

Nikaido, H. (2003) Molecular basis of bacterial outer membrane permeability revisited. *Microbiol Mol Biol Rev* **67:** 593–656.

Oddershede, L., Dreyer, J.K., Grego, S., Brown, S., and Berg-Sorensen, K. (2002) The motion of a single molecule, the lambda-receptor, in the bacterial outer membrane. *Biophys J* **83:** 3152–3161.

Palade, G.E. (1952) A study of fixation for electron microscopy. *J Exp Med* **95:** 285–298.

de Pedro, M.A., Quintela, J.C., Holtje, J.V., and Schwarz, H. (1997) Murein segregation in *Escherichia coli*. *J Bacteriol* **179:** 2823–2834.

Qian, H., Sheetz, M.P., and Elson, E.L. (1991) Single particle tracking. Analysis of diffusion and flow in two-dimensional systems. *Biophys J* **60:** 910–921.

Randall-Hazelbauer, L., and Schwartz, M. (1973) Isolation of the bacteriophage lambda receptor from *Escherichia coli*. *J Bacteriol* **116:** 1436–1446.

Raskin, D.M., and de Boer, P.A. (1999a) MinDE-dependent pole-to-pole oscillation of division inhibitor MinC in *Escherichia coli*. *J Bacteriol* **181:** 6419–6424.

Raskin, D.M., and de Boer, P.A. (1999b) Rapid pole-to-pole oscillation of a protein required for directing division to the middle of *Escherichia coli*. *Proc Natl Acad Sci USA* **96:** 4971–4976.

Rizzitello, A.E., Harper, J.R., and Silhavy, T.J. (2001) Gentle evidence for parallel pathways of chaperone activity in the periplasm of *Escherichia coli*. *J Bacteriol* **183:** 6794–6800.

Robbins, J.R., Monack, D., McCallum, S.J., Vegas, A., Pham, E., Goldberg, M.B., and Theriot, J.A. (2001) The making of a gradient: IcsA (VirG) polarity in *Shigella flexneri*. *Mol Microbiol* **41:** 861–872.

Rodriguez-Torres, A., Ramos-Sanchez, M.C., Orduna-Domingo, A., Martin-Gil, F.J., and Martin-Gil, J. (1993) Differential scanning calorimetry investigations on LPS and free lipids A of the bacterial cell wall. *Res Microbiol* **144:** 729–740.

Ryter, A., Shuman, H., and Schwartz, M. (1975) Integration of the receptor for bacteriophage lambda in the outer membrane of *Escherichia coli*: coupling with cell division. *J Bacteriol* **122:** 295–301.

Sabatini, D.D., Bensch, K., and Barrnett, R.J. (1963) Cytochemistry and electron microscopy. The preservation of cellular ultrastructure and enzymatic activity by aldehyde fixation. *J Cell Biol* **17:** 19–58.

Sandlin, R.C., Lampel, K.A., Keasler, S.P., Goldberg, M.B., Stolzer, A.L., and Maurelli, A.T. (1995) Avirulence of rough mutants of *Shigella flexneri*: requirement of O antigen for correct unipolar localization of IcsA in the bacterial outer membrane. *Infect Immun* **63:** 229–237.

Saxton, M.J. (1997) Single-particle tracking: the distribution of diffusion coefficients. *Biophys J* **72:** 1744–1753.

Scheffers, D., Jones, L.J., and Errington, J. (2004) Several distinct localization patterns for penicillin-binding proteins in *Bacillus subtilis*. *Mol Microbiol* **51:** 749–764.

Schwartz, M. (1976) The adsorption of coliphage lambda to its host: effect of variations in the surface density of receptor and in phage-receptor affinity. *J Mol Biol* **103:** 521–536.

Shapiro, L., McAdams, H.H., and Losick, R. (2002) Generating and exploiting polarity in bacteria. *Science* **298:** 1942–1946.

Shih, Y.L., Le, T., and Rothfield, L. (2003) Division site selection in *Escherichia coli* involves dynamic redistribution of Min proteins within coiled structures that extend between the two cell poles. *Proc Natl Acad Sci USA* **100:** 7865–7870.

Southward, C.M., and Surette, M.G. (2002) The dynamic microbe: green fluorescent protein brings bacteria to light. *Mol Microbiol* **45:** 1191–1196.

Souzu, H. (1986) Fluorescence polarization studies on *Escherichia coli* membrane stability and its relation to the resistance of the cell to freeze-thawing. I. Membrane stability in cells of differing growth phase. *Biochim Biophys Acta* **861:** 353–360.

Steinhauer, J., Agha, R., Pham, T., Varga, A.W., and Goldberg, M.B. (1999) The unipolar *Shigella* surface protein IcsA is targeted directly to the bacterial old pole: IcsP cleavage of IcsA occurs over the entire bacterial surface. *Mol Microbiol* **32:** 367–377.

Studier, F.W., Rosenberg, A.H., Dunn, J.J., and Dubendorff, J.W. (1990) Use of T7 RNA polymerase to direct expression of cloned genes. *Methods Enzymol* **185:** 60–89.

Surana, U., Wolfe, A.J., and Mendelson, N.H. (1988) Regulation of *Bacillus subtilis* macrofiber twist development by D-alanine. *J Bacteriol* **170:** 2328–2335.

Thanassi, D.G., and Hultgren, S.J. (2000) Multiple pathways allow protein secretion across the bacterial outer membrane. *Curr Opin Cell Biol* **12:** 420–430.

Vanounou, S., Parola, A.H., and Fishov, I. (2003) Phosphatidylethanolamine and phosphatidylglycerol are segregated into different domains in bacterial membrane. A study with

pyrene-labelled phospholipids. *Mol Microbiol* **49:** 1067–1079.

Voorhout, W.F., Leunissen-Bijvelt, J.J.M., Leunissen, J.L.M., and Verkleij, A.J. (1986) Steric hindrance in immunolabelling. *J Microsc* **141:** 303–310.

Vos-Scheperkeuter, G.H., Pas, E., Brakenhoff, G.J., Nanninga, N., and Witholt, B. (1984) Topography of the insertion of LamB protein into the outer membrane of *Escherichia coli* wild-type and lac-lamB cells. *J Bacteriol* **159:** 440–447.

Wang, J., Michel, V., Hofnung, M., and Charbit, A. (1998) Cloning of the J gene of bacteriophage lambda, expression and solubilization of the J protein: first *in vitro* studies on the interactions between J and LamB, its cell surface receptor. *Res Microbiol* **149:** 611–624.

Weigle, J. (1968) Studies on head-tail union in bacteriophage lambda. *J Mol Biol* **33:** 483–489.

Wolfe, A.J., and Mendelson, N.H. (1987) Characterization of nutrition-induced helix hand inversion of *Bacillus subtilis* macrofibers. *J Bacteriol* **169:** 4068–4075.